

Successive Change in Conformation Caused by *p*-Y Groups in 1-(MeSe)-8-(*p*-YC₆H₄Se)C₁₀H₆: Role of Linear Se···Se–C Three-Center–Four-Electron versus n(Se)···n(Se) Two-Center–Four-Electron Nonbonded Interactions

Warô Nakanishi,* Satoko Hayashi, and Tetsutaro Uehara†

Department of Material Science and Chemistry, Faculty of Systems Engineering, and Center for Information Science, Wakayama University, 930 Sakaedani, Wakayama 640-8510, Japan

Received: June 10, 1999; In Final Form: September 20, 1999

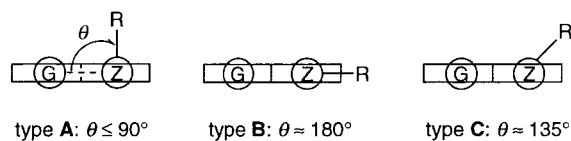
The structure of 1-(methylselanyl)-8-(*p*-anisylselanyl)naphthalene (**2**) and 1-(methylselanyl)-8-(*p*-chlorophenylselanyl)naphthalene (**3**) was studied by X-ray crystallographic analysis. The structures around the Se–Me and Se–C₆H₄OMe-*p* (Se–C_{An}) groups in **2** are close to type A and type B, respectively: type A if the Se–C bond is almost perpendicular to the naphthyl plane and type B when the Se–C bond is placed on the plane. Those around the Se–Me and Se–C₆H₄Cl-*p* (Se–C_{Ar}) groups in **3** are type B and type A, respectively. The nonbonded Se···Se distances of **2** and **3** are 3.0951(8) and 3.1239(7) Å, respectively. The structure of **3** is very different from that observed in 1-(methylselanyl)-8-(phenylselanyl)naphthalene (**1**), the structure of which is type C, where the two Se–C bonds decline by about 45° from the naphthyl plane. The structure of **3** strongly suggests the contribution of the nonbonded n(Se_{Ar})···σ*(Se–C_{Me}) three-center–four-electron (3c–4e) type interaction. The nonbonded n(Se_{Me})···σ*(Se–C_{An}) 3c–4e type interaction must partly contribute to the structure of **2**. To clarify the nature of the n(Se)···σ*(Se–C) 3c–4e type interaction observed in **2** and **3**, together with the π type two-center–four-electron interaction in **1**, ab initio MO calculations with the B3LYP/6-311++G(3df,2pd) method were performed on model a, H_aH_bSe···SeH_aH_b, where the naphthylidene group was replaced by H_a and H_a' and the Me and Ar groups by H_b and H_b'. Two structures are optimized to be energy minima with ∠SeSeH_b = ∠SeSeH_b' = ca. 74° and 155°. The latter corresponds to the conformation observed in **1**, which is controlled by HOMO (π*(Se···Se)); the former is HOMO-1 (σ(Se···Se))-controlled. On the contrary, similar calculations with the B3LYP/6-311+G(2d,p) method on naphthalene-1,8-diselenol show that the type A–type B pairing is evaluated to be most stable, which explains the conformations observed in **2** and **3**: the n(Se)···σ*(Se–C) 3c–4e interaction, as well as π-orbitals of the naphthyl group, play an important role in the pairing. The resonance effect of OMe and the inductive effect of Cl must also be important to determine the structures of **2** and **3**, respectively. The character of CT calculated by the natural population analysis for the diselenol supports further the n(Se)···σ*(Se–C) 3c–4e interaction.

Introduction

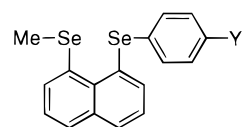
The lone pair–lone pair interaction¹ is one of the important factors to determine the structure and the reactivity of organic compounds containing heteroatoms bearing lone pairs such as organic chalcogen compounds. Such two-center–four electron (2c–4e) interaction is demonstrated to play an important role in the nuclear spin–spin couplings between selenium–selenium^{2,3} and selenium–fluorine⁴ atoms, as well as those between fluorine–fluorine⁵ and fluorine–nitrogen⁶ atoms. Naphthalene 1,8-positions are expected to serve as a good system to study the nonbonded interactions between heteroatoms and/or groups containing 2c–4e.^{2,3,7,8}

We have recently reported the structure of 1-(methylselanyl)-8-(phenylselanyl)naphthalene (**1**)^{8a} studied by the X-ray crystallographic analysis, together with the molecular orbital calculations performed on the models of **1**. The structure of **1** is demonstrated to decline by about 45° from the naphthyl plane, which is called type C for the two Se–C bonds (Scheme 1; The angle θ is defined in type A).^{8a} The nonbonded 2c–4e interaction itself must be repulsive, but the type C pairing is

SCHEME 1



stabilized by the distorted π type 2c–4e interaction. We looked for such nonbonded Se···Se interaction that is attractive in nature and examined the structure of para-substituted derivatives of **1**⁹ such as 1-(methylselanyl)-8-(*p*-anisylselanyl)naphthalene (**2**) and 1-(methylselanyl)-8-(*p*-chlorophenylselanyl)naphthalene (**3**).

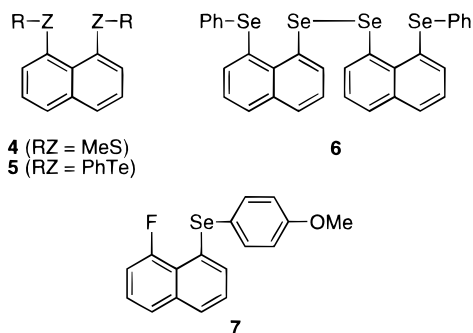


1 (Y = H), **2** (Y = OMe), **3** (Y = Cl)

The type C pairing is usually found in 1,8-bis(chalcogena)-naphthalenes such as **1**, 1,8-bis(methylsulfanyl)naphthalene (**4**),^{7a} and 1,8-bis(phenyltelluro)naphthalene (**5**).^{7b} On the other hand, the double type A–type B pairings are found around the Se–

* Corresponding author. Tel: +81-73-457-8252. Fax: +81-73-457-8253 or +81-73-457-8272. E-mail: nakanishi@sys.wakayama-u.ac.jp.

† Center for Information Science.



Ph and Se–Se moieties in bis [8-(phenylselanyl)naphthyl]-1,1'-diselenide (**6**).⁸ The high electron accepting ability of the Se–Se bond due to the low lying $\sigma^*(\text{Se}–\text{Se})$ bond must be the driving force for the formation of the pairings. Indeed the type C structure is stabilized by the distorted π type $2c–4e$ interaction as in **1**, but the type A-type B pairing must also be stabilized through the electron donor–acceptor interaction. The type B structure was also reported for 8-fluoro-1-(*p*-anisylselanyl)naphthalene (**7**).⁴ However, such type A-type B pairing has not been reported in 1,8-bis(alkyl(or aryl)chalcogena)naphthalenes, yet. In the course of our investigation into the nonbonded $\text{Se}\cdots\text{Se}$ interaction, we encountered a pseudo type A–type B pairing around the Se–Me and Se–C₆H₄OMe-*p* (Se–C_{An}) groups in **2** and a pure type A-type B pairing around the Se–C₆H₄Cl-*p* (Se–C_{Ar}) and Se–Me groups in **3**. This finding led us to clarify the nature of the nonbonded $\text{Se}\cdots\text{Se}$ interaction in the naphthalene system in more detail.

The type A–type B pairing in **3** strongly suggest that the nonbonded $\text{Se}\cdots\text{Se}$ interaction should be characterized by the $n(\text{Se}_{\text{Ar}})\cdots\sigma^*(\text{Se}–\text{C}_{\text{Me}})$ $3c–4e$ interaction.^{10,11} The pseudo type A–type B pairing in **2** also suggests the contribution of the $n(\text{Se}_{\text{Me}})\cdots\sigma^*(\text{Se}–\text{C}_{\text{An}})$ $3c–4e$ interaction. The $\sigma^*(\text{Se}–\text{C})$ bonds in **2** and **3** are to act as electron acceptors. We report the crystal structures of **2** and **3**, together with the nature of the $n(\text{Se})\cdots n(\text{Se})$ interaction in the naphthalene system elucidated by the MO calculations performed on the models of **2** and **3**.

Results and Discussion

Structure of 1-(Methylselanyl)-8-(arylselanyl)naphthalenes, 2 and 3. Single crystals of **2** and **3** were obtained via slow evaporation of hexane solutions, and each of the suitable crystals was subjected to X-ray crystallographic analysis. The crystallographic data are shown in Table 1. One type of structure corresponds to each crystal. Figures 1 and 2 show the structures of **2** and **3**, respectively. Table 2 collects the selected interatomic distances, angles, and torsional angles for **2** and **3**.

Deviations of atoms from the least-squares planes of C(3)–C(4)–C(5)–C(6)–C(7)–C(10) in **2** and **3** are shown in Table 3, together with those of **1A** and **1B**.^{8a} The planarity of the plane in **2** is good and that in **3** is very good. The Se(1), C(1), and C(2) atoms deviate from the planes in the minus direction, and the Se(2), C(8), and C(9) atoms in the opposite direction. Deviations of the Se atoms in **2** are in a range of 0.50–0.64 Å, while the atoms in **3** deviate only 0.20 ± 0.02 Å. The deviations of atoms are in an order of **3** < **1** < **2**.

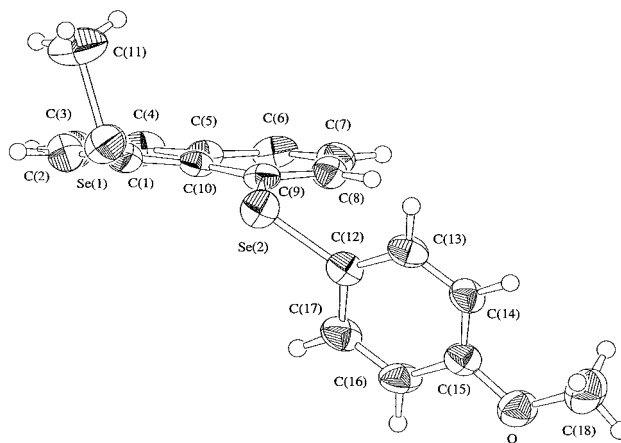
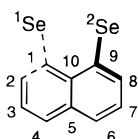


Figure 1. Structure of **2**.

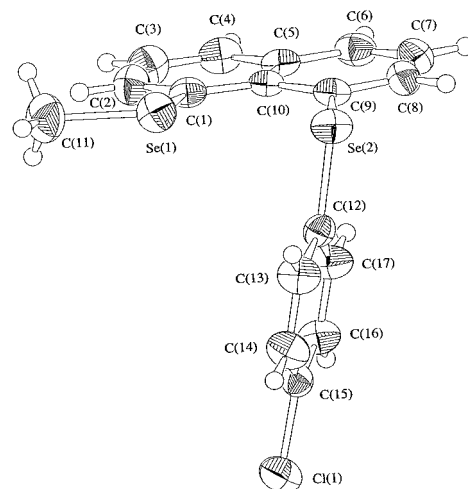


Figure 2. Structure of **3**.

TABLE 1: Selected Crystal Data and Structure Refinement for **2** and **3**

	2	3
formula	C ₁₈ H ₁₆ O ₁ Se ₂	C ₁₇ H ₁₃ Cl ₁ Se ₂
fw (g mol ⁻¹)	406.24	410.66
crystal color and habit	colorless, prismatic	pale yellow, cubic
crystal system	monoclinic	triclinic
space group	<i>P</i> 2 ₁ / <i>n</i> (No. 14)	<i>P</i> $\bar{1}$ (No. 2)
unit cell dimens	<i>a</i> = 12.754(2) Å <i>b</i> = 9.804(1) Å <i>c</i> = 12.980(2) Å	<i>a</i> = 9.628(4) Å <i>b</i> = 10.901(3) Å <i>c</i> = 8.565(2) Å
	β = 96.68(1)°	α = 111.90(2)° β = 96.55(3)° γ = 109.99(3)°
vol (Å ³)	1611.8(3)	753.1(5)
<i>Z</i>	4	2
density (calcd) (g cm ⁻³)	1.674	1.811
$\mu(\text{Mo K}\alpha)$ (cm ⁻¹)	45.84	50.74
<i>F</i> (000)	800.00	400.00
scan width (deg)	1.00 + 0.30 tan θ	1.20 + 0.30 tan θ
2 θ_{max} (deg)	55.0	55.0
no. of observations	2331	2754
no. of variables	191	182
<i>R</i>	0.042	0.030
<i>R</i> _w	0.030	0.023
GOF	2.51	2.93

As shown in Figure 1 and Table 2, the Se–C_{Me} and Se–C_{An} bonds in **2** decline by about 73° and 34° from the naphthyl plane, respectively: the torsional angles of C(10)–C(1)–Se(1)–C(11) and C(10)–C(9)–Se(2)–C(12) were 107.1(4)° and 145.7(4)°, respectively. The *p*-anisyl plane was slightly declined from the naphthyl plane: the torsional angle of C(9)–Se(2)–C(12)–

TABLE 2: Selected Interatomic Distances, Angles, and Torsional Angles of **2 and **3****

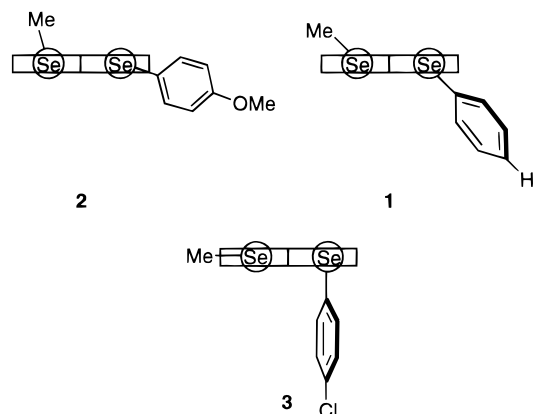
	2	3
Interatomic Distances, Å		
Se(1)–C(1)	1.932(5)	1.926(3)
Se(1)–C(11)	1.931(5)	1.954(3)
Se(2)–C(9)	1.951(4)	1.924(3)
Se(2)–C(12)	1.928(5)	1.915(3)
Se(1)–Se(2)	3.0951(8)	3.1239(7)
C(1)–C(10)	1.422(6)	1.435(3)
C(9)–C(10)	1.432(6)	1.433(3)
Angles, deg		
C(1)–Se(1)–C(11)	53.8(2)	69.8(1)
Se(1)–C(1)–C(10)	122.6(4)	123.0(2)
C(9)–Se(2)–C(12)	98.2(2)	98.8(1)
Se(2)–C(9)–C(10)	121.8(3)	122.3(6)
C(1)–C(10)–C(9)	127.1(4)	125.3(2)
Se(1)–Se(2)–C(12)	166.6(2)	87.28(8)
Se(2)–Se(1)–C(11)	129.3(2)	172.2(1)
Torsional Angles, deg		
C(10)–C(1)–Se(1)–C(11)	107.1(4)	180.0(2)
Se(1)–C(1)–C(10)–C(9)	14.9(7)	4.8(4)
C(2)–C(1)–Se(1)–C(11)	–66.2(5)	1.7(2)
C(10)–C(9)–Se(2)–C(12)	145.7(4)	78.4(2)
Se(2)–C(9)–C(10)–C(1)	13.4(7)	5.0(4)
C(9)–Se(2)–C(12)–C(13)	110.1(4)	–165.5(2)
C(9)–Se(2)–C(12)–C(17)	–74.7(4)	14.8(3)
C(8)–C(9)–Se(2)–C(12)	–30.0(4)	–99.5(2)
C(11)–Se(1)–Se(2)–C(12)	38.6(2)	–23.8(7)
C(2)–C(1)–C(10)–C(5)	–9.2(7)	–2.6(4)
C(5)–C(10)–C(9)–C(8)	–7.6(6)	–3.2(4)

C(13) was 110.1(4)°. The structures around the Se–C_{Me} and Se–C_{An} bonds in **2** were close to type A and type B, respectively, bearing some type C character. The nonbonded Se(1)···Se(2) distance was 3.0951(8) Å, which was almost equal to that in **1** [3.048(1) and 3.091(1) Å for the two structures].^{8a} The type A and type B structures around the Se–C_{Ar} and Se–C_{Me} bonds were demonstrated for **3** (Figure 2 and Table 2). The Se–C_{Me} and Se–C_{Ar} bonds in **3** decline by about 0° and 78° from the naphthyl plane, respectively: the torsional angles of C(10)–C(1)–Se(1)–C(11) and C(10)–C(9)–Se(2)–C(12) were 180.0(2)° and 78.4(2)°, respectively. The *p*-chlorophenyl plane was almost perpendicular to the naphthyl plane: the torsional angle of C(9)–Se(2)–C(12)–C(13) was –165.5(2)°. The nonbonded Se(1)···Se(2) distance was 3.1239(7) Å, which was somewhat longer than those of **1** [3.048(1) and 3.091(1) Å for the two structures]^{8a} and **2** [3.0951(8) Å]. It is worthwhile to note that the Se–Me groups in **2** and **3** are shown to be type A and type B, respectively. Their inverse contribution to the structures must be due to the difference in the electronic effect of the para-substituents in **2** and **3**.

Parthasarathy et al. have suggested that there are two types of directional preferences of nonbonded atomic contacts with divalent chalcogens such as sulfur¹² and selenium,¹³ R–Z–R' (Z = S and Se). Type I contacts are with electrophiles which have Z···X directions in RR'Z···X where n-electrons of sulfides or selenides are located, and type II contacts are with nucleophiles tending to lie along the extension of one of the sulfur or

selenium bonds. Electrophiles and nucleophiles will interact preferentially with HOMO of the n(Z) and with LUMO of the σ*(Z–R) or σ*(Z–R'), respectively. Therefore, the type A and type B structures belong to type I and type II contacts in Parthasarathy's definition, respectively, if G in 8-G-1-(RZ)C₁₀H₆ is assumed to be an electrophile or nucleophile (Scheme 1). The type A–type B pairing is equal to the type I–type II pairing, which is stabilized through the electron donor–acceptor interaction. The type C structure around the two chalcogen atoms must be equal to the type III pairing, for which θ values at the both sites should be almost equal.

The conformations around the Se–C_{Ar} and Se–C_{Me} bonds in **3** are demonstrated to be type A and type B, respectively, which is also recognized as the type I–type II pairing in Parthasarathy's classification. Since the type I and type II contacts are with LUMO and HOMO, respectively, the type I–type II pairing must be the HOMO–LUMO interaction. The pairing must be stabilized by the charge transfer (CT) from the electron donor to the acceptor. That is, the pairing in **3** strongly suggests that the interaction occurs between the n(Se) of the ArSe group and the σ*(Se–C) of the MeSe group, which leads to the n(Se_{Ar})···σ*(Se–C_{Me}) 3c–4e type interaction.^{10,11} The pairing in **2** also suggests the contribution of the n(Se_{Me})···σ*(Se–C_{An}) 3c–4e type, together with the contribution of the distorted π type 2c–4e interaction. The type C pairing of the distorted π type 2c–4e interaction is reported for **1**. The three structures show that the pairing changes successively with the substituent Y at the para-position in **1–3**.



Why does the type C pairing in **1** change successively and/or dramatically to the type A–type B pairing in **2** and **3**, respectively? Three types of interactions between nonbonded Se···Se atoms in **1–3** should be considered for the successive change: (i) pure n(Se)···n(Se) 2c–4e interaction, (ii) n(Se)···σ*(Se–C) 3c–4e interaction, and (iii) contribution of the methyl and aryl groups, especially of π-orbitals of the naphthylidene group. The role of the substituents OMe and Cl at the phenyl para-positions is also important. Ab initio MO calculations are performed on an adduct, H₂Se···SeH₂ (model a), to clarify the contributions of cases i and ii, together with

TABLE 3: Deviations of Atoms from Least-Squares Planes of C(3)–C(4)–C(5)–C(6)–C(7)–C(10)^{a,b} in **1–3**

compd	Se(1)	Se(2)	C(1)	C(2)	C(8)	C(9)	C(3)	C(4)	C(5)	C(6)	C(7)	C(10)
2	–0.644	0.500	–0.134	–0.119	0.103	0.134	–0.007(5)	0.009(5)	0.001(5)	–0.011(5)	0.007(5)	–0.001(4)
3	–0.183	0.220	–0.050	–0.039	0.043	0.058	–0.003(3)	0.004(3)	0.000(3)	–0.004(3)	0.003(3)	0.000(2)
1A^c	0.366	–0.372	0.075	0.019	–0.088	–0.088	–0.022(9)	0.010(9)	0.013(7)	0.006(9)	–0.02(1)	0.003(7)
1B^c	0.398	–0.407	0.074	0.015	–0.112	–0.108	–0.025(9)	0.011(9)	0.012(8)	0.011(9)	–0.03(1)	0.004(7)

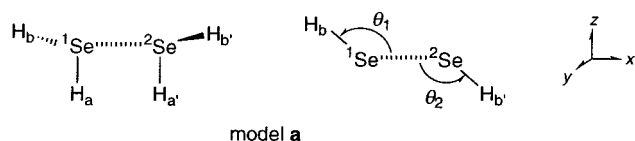
^a In Å. ^b Conformations around MeSe and *p*-YC₆H₄Se groups in **2** and **3** are just the opposite of those in **1**. ^c Based on the structures in ref 8a.

TABLE 4: Optimized Structures, Energies, and Natural Charges (Qn) for Model a and 8

compd	<i>E</i> (au)	structure	<i>r</i> (Se,Se) (Å)	$\angle H_a H_a^1 Se H_b$ (deg)	$\angle H_a^1 Se H_b$ (deg)	Qn(¹ Se)	Qn(H _a)	Qn(H _b)
B3LYP/6-311++G(3df,2pd)								
model a	-4805.4884	C ₂	3.124 ^a	74.29	91.62	-0.1650	0.0812	0.0839
model a	-4805.5072	C ₂	3.124 ^a	154.54	90.04	-0.1620	0.0837	0.0783
model a	-4805.5057	C _{2v}	3.124 ^a	180.00 ^b	90.44	-0.1752	0.0845	0.0908
model a	-4805.5052	C ₁	3.124 ^a	90.00 ^a	91.24	-0.1229	0.0865	0.0905
				181.36 ^c	88.93 ^d	-0.1854 ^e	0.0789 ^f	0.0524 ^g
B3LYP/6-311+G(2d,p)								
8a ^{h,i}	-5189.0663	C ₂	3.5166	52.99	97.87	0.0993	-0.1829	0.0948
8b ^{h,i}	-5189.0709	C ₂	3.1173	143.11	92.44	0.1330	-0.1699	0.0696
8c ^{h,j}	-5189.0684	C _{2v}	3.1047	180.00	93.13	0.1449	-0.1660	0.0768
8d ^{h,i}	-5189.0714	C ₁	3.1806	72.82	95.51	0.1310	-0.1871	0.0902
				172.84 ^k	91.14 ^l	0.1490 ^e	-0.1695 ^m	0.0398 ^g

^a Fixed value. ^b $\angle H_a H_a^2 Se H_b$ being optimized with $\angle H_a H_a^1 Se H_b$ fixed at 180.00°. ^c $\angle H_a H_a^2 Se H_b$. ^d $\angle H_a^2 Se H_b$. ^e Qn(²Se). ^f Qn(H_a). ^g Qn(H_b). ^h H_a and H_a² should be read C₁ and C₉, respectively. ⁱ All positive frequencies being predicted by the frequency analysis. ^j Three negative frequencies being predicted by the frequency analysis. ^k $\angle C_1 C_9^2 Se H_b$. ^l $\angle C_9^2 Se H_b$. ^m Qn(C₉).

SCHEME 2



the whole nature of the nonbonded n(Se)···n(Se) interaction. Calculations are also performed on naphthalene-1,8-diselenol (**8**) to elucidate the contributions of cases ii and iii. The results are shown in the following sections.

Ab Initio MO Calculations on Model a. Scheme 2 shows model a, H_aH_b¹Se···²SeH_aH_b, where aryl, methyl, and naphthylidene groups are replaced by hydrogens. The ¹Se atom of model a is placed at the origin and the ²Se atom on the *x*-axis with the ¹Se···²Se distance fixed at 3.124 Å and the ¹Se–H_a and ²Se–H_a bonds in the *z*-direction. Ab initio MO calculations were performed on model a using the Gaussian94 program¹⁴ with the 6-311++G(3df,2pd) basis sets at the B3LYP level. The results are shown in Table 4.

Two structures of the C₂ symmetry were optimized to be energy minima, the torsional angle H_aH_a¹SeH_b (θ_1) of which were $\theta_1(=\theta_2) = 74.29^\circ$ and 154.54° ; the former (model a with $\theta = 74.3^\circ$) is less stable than the latter (model a with $\theta = 154.5^\circ$) by 0.0188 au (49.4 kJ mol⁻¹).¹⁵ The former corresponds to the type A pairing with the nonbonded σ type 2c–4e interaction and the latter to type C pairing with the nonbonded π type 2c–4e interaction observed in **1**.

To clarify the whole nature of the nonbonded interaction between Se atoms, the angular dependence of the energy of model a is calculated with variously fixed θ_1 . The partial optimization of model a with a fixed value of θ_1 , yields energies *E* (*E*₁ and *E*₂) and angles θ_2 (θ_{21} and θ_{22}). The energies *E*₁ and *E*₂ represent those obtained when θ_2 is started near 154° and 74°, respectively, with a fixed θ_1 . The values of *E*₁ and the corresponding θ_{21} are obtained for a trial range of $60^\circ \leq \theta_1 \leq 180^\circ$, while the *E*₂ value, together with θ_{22} , is found in a range of $60^\circ \leq \theta_1 < 120^\circ$. The energies *E*₁ and *E*₂ are on different energy curves, which cross at $\theta_2 = \text{ca. } 120^\circ$: *E*₂ is represented by *E*₁, if *E*₁ = *E*₂. For example, θ_{21} and θ_{22} are optimized to be 181.36° and 73.03°, respectively, when calculations are carried out with θ_1 fixed at 90.00°. In the case where θ_1 is fixed at 180.00°, two structures are optimized: the one is $\theta_{21} = 180.00^\circ$ when calculations are started at $\theta_{21} = 180.0^\circ$ and the other is $\theta_{21} = 155.33^\circ$ starting with $\theta_{21} = 179.0^\circ$. The former may not be an energy minimum. Figures 3 and 4 show the plots of *E* and θ_2 versus θ_1 , respectively.

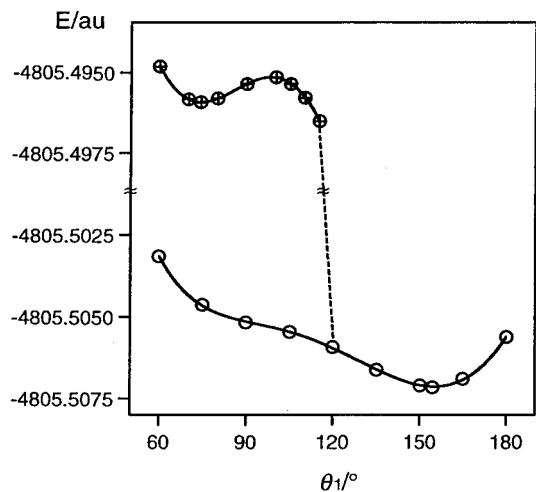


Figure 3. Plots of *E*₁ and *E*₂ of model a against θ_1 : ○ and ⊗ stand for *E*₁ and *E*₂, respectively.

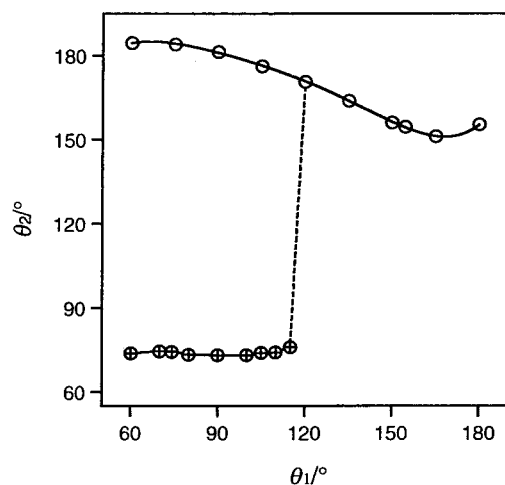


Figure 4. Plots of θ_{21} and θ_{22} of model a against θ_1 : ○ and ⊗ stand for θ_{21} and θ_{22} , respectively.

Why do the *E*₁ and *E*₂ curves contain energy minima at $\theta_1 = \theta_2 = 154.54^\circ$ and 74.29° , respectively? The energies of the HOMO and HOMO-1 are plotted against θ_1 , which is shown in Figure 5. The HOMO of *E*₁ shows a minimum at near $\theta_1 = \theta_{21} = 154.5^\circ$, whereas its HOMO-1 changes rather monotonically with θ_1 . On the other hand, the HOMO and HOMO-1 of *E*₂ exhibit a maximum and a minimum at near $\theta_1 = \theta_{22} = 74.3^\circ$, respectively. The HOMO curve is more flat than that of HOMO-

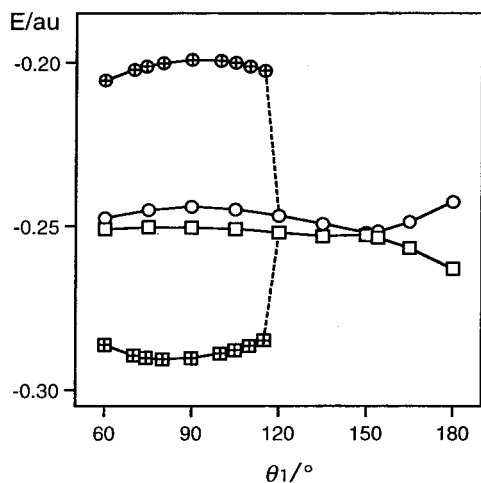


Figure 5. Plots of the energies of HOMO and HOMO-1 for E_1 and E_2 of model a against θ_1 : \circ and \otimes stand for HOMO of E_1 and E_2 , respectively, and \square and \boxtimes for HOMO-1 of E_1 and E_2 , respectively.

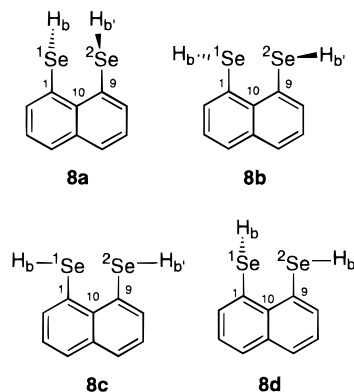
1, in this case. These results show that the presence of minima on E_1 and E_2 is the reflection of the characters of HOMO of E_1 and HOMO-1 of E_2 , respectively. Consequently, E_1 and E_2 are demonstrated to be HOMO- and HOMO-1-controlled,¹⁶ respectively.

Molecular orbitals were depicted using the MacSpartan program¹⁷ with 3-21G(*) basis sets employing the structures given in Table 4. Figure 6 shows HOMO and HOMO-1 of model a with $\theta = 74.3^\circ$ (a), 154.5° (b), 180.0° (c), and $(\theta_1, \theta_2) = (90.0^\circ, 181.4^\circ)$ (d). Characters of the interactions are σ type 2c-4e (a), distorted π type 2c-4e (b), undistorted π type 2c-4e (c), and $n(\text{Se})\cdots\sigma^*(\text{Se}-\text{H})$ type 3c-4e interactions (d) between the nonbonded $\text{Se}\cdots\text{Se}$ atoms. Model a with $(\theta_1, \theta_2) = (90.0^\circ, 181.4^\circ)$ (d) is less stable than that with $\theta = 154.5^\circ$ (b) by 0.0020 au (5.3 kJ mol⁻¹) and slightly less stable than that with $\theta = 180.0^\circ$ (c) by 0.0005 au (1.3 kJ mol⁻¹). The electron donor-acceptor interaction does not effectively contribute to the $n(\text{Se})\cdots n(\text{Se})$ interaction in model a, although that with $(\theta_1, \theta_2) = (90.0^\circ, 181.4^\circ)$ (d) is more stable than that with $\theta = 74.3^\circ$ (a) by 0.0168 au (44.1 kJ mol⁻¹).

It is worthwhile to note that the explicit nodal plane in the undistorted π^* orbital between the nonbonded $\text{Se}\cdots\text{Se}$ atoms disappears in the distorted π^* orbital (Figure 6). The disappearance of the nodal plane between the two Se atoms must stabilize model a with $\theta = 154.5^\circ$, which may avoid the severe exchange repulsion of the π type 2c-4e interaction more effectively^{8a} and be the driving force for the type C pairing in

1, 4, and 5. The disappearance of the nodal plane in the distorted π type 2c-4e interaction may remember the Möbius type interaction in cyclic π systems. We call it "Möbius type stabilization in the distorted π type 2c-4e interaction", although the π type 2c-4e interaction does not form a ring.

Ab Initio MO Calculations on 8. Table 4 collects the results of MO calculations performed on **8**¹⁸ with the B3LYP/6-311+G-(2d,p) method. The optimized structures of **8** are shown by **8a-d**, of which $(\theta_1, \theta_2) = (52.99^\circ, 52.99^\circ)$, $(143.11^\circ, 143.11^\circ)$,



$(180.00^\circ, 180.00^\circ)$, and $(72.82^\circ, 172.84^\circ)$, respectively, where θ_1 and θ_2 are defined as torsional angles of $\text{C}_9\text{C}_1^1\text{SeH}_b$ and $\text{C}_1\text{C}_9^2\text{SeH}_b$, respectively. Although all positive frequencies are predicted by the frequency analysis for **8a**, **8b**, and **8d**, three negative frequencies are predicted for **8c**, which is optimized when calculations are carried out assuming the C_{2v} symmetry. The conformer **8d** is most stable, which is a striking difference from the case of model a: **8d** is more stable than **8a** and **8b** by 0.0051 au (13.4 kJ mol⁻¹) and 0.0005 au (1.3 kJ mol⁻¹), respectively. The HOMO and HOMO-1 of **8a-d** are essentially the same as those of model a shown by parts a-d in Figure 6, respectively.

The most stable structure in model a with $\theta = 154.5^\circ$ changes to **8d**. The large energy difference between model a with $\theta = 154.5^\circ$ and that with $\theta = 74.3^\circ$ (0.0188 au) decreases to 0.0046 au between **8b** and **8a**, which must be not only due to the interaction with the π orbitals of the naphthalene ring but also due to the increased $\text{Se}\cdots\text{Se}$ distance in **8a**. Model a with $\theta = 154.5^\circ$, together with **8b**, and **8d** correspond to those of **1** and **3**, respectively. The results show that the structures of **1** and **3** are mainly governed by the π type 2c-4e^{8a} and the $n(\text{Se})\cdots\sigma^*(\text{Se}-\text{C})$ 3c-4e interactions with the aid of the π orbitals of the naphthalene ring. The aryl and methyl groups in **1-3** must

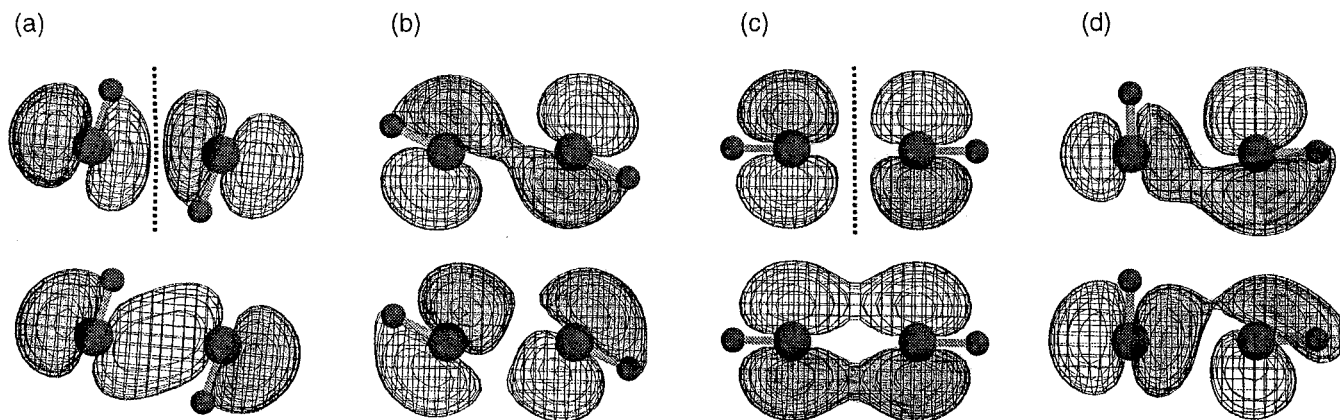


Figure 6. HOMO (upper) and HOMO-1 (lower) of model a with $\theta = 74.3^\circ$ (a), with $\theta = 154.5^\circ$ (b), with $\theta = 180.0^\circ$ (c), and with $(\theta_1, \theta_2) = (90.0^\circ, 181.4^\circ)$ (d). The nodal planes are shown by dotted lines for parts a and c.

also play an important role in determining the structures, since the energy difference between **8b** and **8d** is so small.

The magnitude of CT is a good measure to gauge the nature of the nonbonded interaction between Se atoms. Natural charges (Qn) were calculated for the conformers of model a and **8**, applying the natural population analysis.¹⁹ The results are also collected in Table 4. The Qn(¹Se), Qn(²Se), and Qn(H_b) values in model a with (θ₁, θ₂) = (90.0°, 181.4°) were calculated to be more positive, negative, and negative, respectively, relative to corresponding values in model a with θ = 74.3° and that with 180.0°. The changes amount to 0.042 [=Qn(¹Se) of model a with (θ₁, θ₂) = (90.0°, 181.4°) - Qn(¹Se) of that with θ = 74.3°], -0.010, and -0.038, respectively. The total CT from an H₂Se molecule to another amounts to 0.054, which shows the large contribution of the n(¹Se)···σ*(²Se-H_b) 3c-4e type interaction in this structure. Similarly, changes in Qn(¹Se), Qn(²Se), and Qn(H_b) in **8d** from the corresponding values in **8a** and **8c** are 0.032, 0.004, and -0.037, respectively, whereas those for other atoms were less than 0.005. The results are in accordance with the large contribution of the n(¹Se)···σ*(²Se-H_b) 3c-4e interaction also in **8d**.

The change in the structure of **1** to those of **2** and **3** in crystals must be accounted for on the basis of the electronic properties of the MeO and Cl groups at the para-positions. Both substituents withdraw electrons inductively [σ_I(OMe) = 0.27 and σ_I(Cl) = 0.46], but they donate electrons by the resonance mechanism [σ_R^o(OMe) = -0.45 and σ_R^o(Cl) = -0.23].²⁰ Since the magnitude of the substituent effects is different for MeO and Cl groups, the observed effect on the structures can be the inverse for the two groups if the resonance effect of OMe in **2** and the inductive effect of Cl in **3** are predominant in the structures. The electron-donating ability of the *p*-anisyl and *p*-chlorophenyl groups is expected to be larger and smaller than that of the methyl group in these cases, judging from their structures.

The character of the structures of **1-3** is summarized as follows: (a) The contribution of the n(Se)···n(Se) π type 2c-4e interaction is predominant in **1** and negligible in **3**;²¹ (b) the n(Se)···σ*(Se-C) 3c-4e type interaction contributes to the structures of **2** and **3**; and (c) the interaction between Se and Y²² through the π-orbitals of the SeC₆H₄Y group determines which Se atom (or Se-C bond) in **2** or **3** acts as an electron donor (or an acceptor) in the 3c-4e interaction.²³ The structures of **1-3** are well-explained by the MO calculations on model a and **8**. The steric effect between the naphthyl protons at the 7- and/or 2-positions and the *p*-YC₆H₄ and/or Me groups in type B must also be taken into account when the structures are discussed in more detail. Studies on the structures of 8-G-1-(RSe)C₁₀H₆ are in progress.

Experimental Section

Chemicals were used without further purification unless otherwise noted. Solvents were purified by standard methods. Melting points were uncorrected. ¹H, ¹³C, and ⁷⁷Se NMR spectra were measured at 400, 100, and 76 MHz, respectively. The ¹H, ¹³C, and ⁷⁷Se chemical shifts are given in ppm relative to those of internal CHCl₃, a slight contaminant in the CDCl₃ solvent, internal CDCl₃ in the solvent, and external MeSeMe, respectively. Column chromatography was performed on silica gel (Fujisilysia BW-300) and acidic alumina (E. Merck).

1-(Methylselanyl)-8-(*p*-methoxyphenylselanyl)naphthalene (2). Bis[8-(*p*-methoxyphenylselanyl)naphthyl]-1,1'-diselenide (**9**) was reduced by NaBH₄ in an aqueous THF and then allowed to react with methyl iodide to give **2** as a colorless

solid, similarly to the case for **1**:^{8a} 91% yield; mp 86.0–87.0 °C; ¹H NMR (CDCl₃, 400 MHz) 2.38 (s, 3H, *J*(Se,H) = 13.4 Hz), 3.79 (s, 3H), 6.83 (dd, 2H, *J* = 8.6 and 2.2 Hz), 7.17 (t, 1H, *J* = 7.7 Hz), 7.33 (t, 1H, *J* = 7.7 Hz), 7.45 (dd, 2H, *J* = 8.1 and 2.2 Hz), 7.45 (dd, 1H, *J* = 6.8 and 1.1 Hz), 7.64 (dd, 1H, *J* = 8.1 and 1.0 Hz), 7.70 (dd, 1H, *J* = 8.0 and 1.1 Hz), 7.79 (dd, 1H, *J* = 7.3 and 1.1 Hz); ¹³C NMR (CDCl₃, 100 MHz) 13.90 (¹*J* = 71.2 Hz, ⁵*J* = 15.7 Hz), 55.23, 115.17, 124.73, 125.70, 125.84, 128.26, 128.75, 131.25, 133.10, 133.50, 133.64, 134.94, 135.80, 136.47 (²*J* = 11.5 Hz), 159.69; ⁷⁷Se NMR (CDCl₃, 76 MHz) 424.5, 233.1 (⁴*J*(Se,Se) = 341.6 Hz). Anal. Calcd for C₁₈H₁₆Se₂O₁: C, 53.22; H, 3.97. Found: C, 53.35; H, 3.90.

1-(Methylselanyl)-8-(*p*-chlorophenylselanyl)naphthalene (3). Following a method similar to that for **2**, **3** was obtained starting from bis[8-(*p*-chlorophenylselanyl)naphthyl]-1,1'-diselenide (**10**) in 87% yield as a colorless solid: mp 78.5–79.5 °C; ¹H NMR (CDCl₃, 400 MHz) 2.34 (s, 3H, *J*(Se,H) = 13.9 Hz), 7.19 (dd, 2H, *J* = 8.6 and 2.2 Hz), 7.24 (t, 1H, *J* = 7.7 Hz), 7.31 (dd, 2H, *J* = 8.8 and 2.2 Hz), 7.36 (t, 1H, *J* = 7.7 Hz), 7.60 (dd, 1H, *J* = 7.3 and 1.5 Hz), 7.71 (dd, 1H, *J* = 7.1 and 1.2 Hz), 7.73 (dd, 1H, *J* = 6.8 and 1.1 Hz), 7.74 (dd, 1H, *J* = 7.3 and 1.2 Hz); ¹³C NMR (CDCl₃, 100 MHz) 13.43 (¹*J* = 72.8 Hz, ⁵*J* = 15.7 Hz), 125.96, 125.99, 128.42, 129.49, 130.86, 131.72, 132.67, 133.50, 133.60, 134.49 (²*J* = 12.4 Hz), 135.26, 135.59, 135.83; ⁷⁷Se NMR (CDCl₃, 76 MHz) 431.6, 234.7 (⁴*J*(Se,Se) = 316.7 Hz). Anal. Calcd for C₁₇H₁₃Se₂Cl₁: C, 49.72; H, 3.19. Found: C, 49.77; H, 3.23.

Bis[8-(*p*-methoxyphenylselanyl)naphthyl]-1,1'-diselenide (9). To a solution of the dianion of naphtho[1,8-*c,d*]-1,2-diselenole, which was prepared by reduction of the diselenole with NaBH₄ in an aqueous THF, was added *p*-methoxybenzenediazonium chloride at low temperature. After the usual workup, the solution was chromatographed on silica gel containing acidic alumina. Recrystallization of the chromatographed product from hexane gave **9** as a yellow solid: 69% yield; mp 143.5–145.0 °C; ¹H NMR (CDCl₃, 400 MHz) 3.74 (s, 6H), 6.75 (dd, 4H, *J* = 8.9 and 2.6 Hz), 7.18 (t, 2H, *J* = 7.8 Hz), 7.32 (t, 2H, *J* = 7.6 Hz), 7.32 (dd, 4H, *J* = 9.0 and 2.7 Hz), 7.67 (dd, 2H, *J* = 8.0 and 0.9 Hz), 7.79 (dd, 2H, *J* = 8.1 and 1.0 Hz), 7.86 (dd, 2H, *J* = 7.2 and 1.4 Hz), 8.14 (dd, 2H, *J* = 7.5 and 1.0 Hz); ¹³C NMR (CDCl₃, 22.4 MHz) 55.27, 115.06, 125.28, 125.82, 126.52, 128.33, 129.78, 130.25, 130.57, 132.74, 133.42, 135.39, 136.14, 137.39, 159.24; ⁷⁷Se NMR (CDCl₃, 68.68 MHz) 416.2, 541.4 (⁴*J*(Se,Se) = 371.6 Hz). Anal. Calcd for C₃₄H₂₆O₂Se₄: C, 52.19; H, 3.35. Found: C, 52.45; H, 3.36.

Bis[8-(*p*-chlorophenylselanyl)naphthyl]-1,1'-diselenide (10). In a method similar to that for **9**, **10** was given, starting from the dianion of naphtho[1,8-*c,d*]-1,2-diselenole and *p*-methoxybenzenediazonium chloride: 68% yield as a yellow solid; mp 185.0–186.0 °C; ¹H NMR (CDCl₃, 400 MHz) 7.13 (br s, 8H), 7.16 (t, 2H, *J* = 7.8 Hz), 7.38 (t, 2H, *J* = 7.7 Hz), 7.70 (dd, 2H, *J* = 8.0 and 0.8 Hz), 7.88 (dd, 2H, *J* = 8.2 and 1.1 Hz), 7.94 (dd, 2H, *J* = 7.2 and 1.3 Hz), 8.02 (dd, 2H, *J* = 7.5 and 1.1 Hz); ¹³C NMR (CDCl₃, 22.4 MHz) 125.95, 126.75, 127.26, 128.43, 129.42, 130.19, 131.28, 131.65, 132.48, 132.91, 133.82, 135.62, 136.36, 139.01; ⁷⁷Se NMR (CDCl₃, 68.68 MHz) 429.1, 534.7 (⁴*J*(Se,Se) = 330.1 Hz). Anal. Calcd for C₃₂H₂₀Se₄Cl₂: C, 48.58; H, 2.55. Found: C, 48.77; H, 2.56.

X-ray Structural Determination. The intensity data were collected on a Rigaku AFC5R four-circle diffractometer with graphite-monochromated Mo Kα radiation (λ = 0.71069 Å) for **2** and **3**. The structures of **2** and **3** were solved by heavy-atom Patterson methods, PATTY,²⁴ and expanded using Fourier

techniques, DIRDIF94.²⁵ All the non-hydrogen atoms were refined anisotropically. Hydrogen atoms were included but not refined. The final cycle of full-matrix least-squares refinement was based on a total of 2331 reflections for **2** and on 2754 for **3**, with 191 observed reflections [$I > 1.50\sigma(I)$] for **2** and 182 for **3**. Variable parameters and converged with unweighted and weighted agreement factors of $R = (\sum||F_o| - |F_c||)/\sum|F_o|$ and $R_w = \{\sum\omega(|F_o| - |F_c|)^2/\sum\omega F_o^2\}^{1/2}$ were used. For least squares, the function minimized was $\sum\omega(|F_o| - |F_c|)^2$, where $\omega = (\sigma_c^2|F_o| + p^2|F_o|^2/4)^{-1}$. Crystallographic details are listed in Table 1.

MO Calculations. Ab initio molecular orbital calculations were performed on an Origin computer using the Gaussian94 program with 6-311++G(3df,2pd) basis sets at the DFT (B3LYP) level on model a. The B3LYP/6-311+G(2d,p) method was employed for the calculations of **8**. The molecular orbitals were drawn by a Power Macintosh 8500/180 personal computer using the MacSpartan Plus program (Ver. 1.0) with 3-21G^(*) basis sets.

Acknowledgment. This work was supported by a Grant-in-Aid for Scientific Research (C) (No. 09640635) (W.N.) and that on Priority Areas (A) (No. 09640635 and 11120232) (W.N.) from Ministry of Education, Science, Sports and Culture, Japan.

Supporting Information Available: X-ray structural information on **2** and **3**. This information is available free of charge via the Internet at <http://pubs.acs.org>.

References and Notes

- (1) (a) Asmus, K.-D. *Acc. Chem. Res.* **1979**, *12*, 436. Musker, W. K. *Acc. Chem. Res.* **1980**, *13*, 200. (b) Bernardi, F.; Csizmadia, I. G.; Mangini, A. (Eds.) *Organic Sulfur Chemistry: Theoretical and Experimental Advances*; Elsevier Scientific, Amsterdam, 1985. (c) Patai, S.; Rappoport, Z. (Eds.) *The Chemistry of Organic Selenium and Tellurium Compounds*; John-Wiley and Sons: New York, 1986; Vol. 1. See also refs cited therein.
- (2) Fujihara, H.; Saito, R.; Yabe, M.; Furukawa, N. *Chem. Lett.* **1992**, 1437.
- (3) (a) Nakanishi, W.; Hayashi, S.; Yamaguchi, H. *Chem. Lett.* **1996**, 947. (b) Hayashi, S.; Nakanishi, W. *J. Org. Chem.* **1999**, *64*, 6688.
- (4) Nakanishi, W.; Hayashi, S.; Sakaue, A.; Ono, G.; Kawada, Y. *J. Am. Chem. Soc.* **1998**, *120*, 3635.
- (5) (a) Mallory, F. B. *J. Am. Chem. Soc.* **1973**, *95*, 7747. (b) Mallory, F. B.; Mallory, C. W.; Fedarko, M.-C. *J. Am. Chem. Soc.* **1974**, *96*, 3536. (c) Mallory, F. B.; Mallory, C. W.; Ricker, W. M. *J. Am. Chem. Soc.* **1975**, *97*, 4770. Mallory, F. B.; Mallory, C. W.; Ricker, W. M. *J. Org. Chem.* **1985**, *50*, 457. Mallory, F. B.; Mallory, C. W.; Baker, M. B. *J. Am. Chem. Soc.* **1990**, *112*, 2577. (d) Ernst, L.; Ibrom, K. *Angew. Chem. Int. Ed. Engl.* **1995**, *34*, 1881. Ernst, L.; Ibrom, K.; Marat, K.; Mitchell, R. H.; Bodwell, G. J.; Bushnell, G. W. *Chem. Ber.* **1994**, *127*, 1119.
- (6) Mallory, F. B.; Luzik, E. D., Jr.; Mallory, C. W.; Carroll, P. J. *J. Org. Chem.* **1992**, *57*, 366. Mallory, F. B.; Mallory, C. W. *J. Am. Chem. Soc.* **1985**, *107*, 4816.
- (7) (a) Glass, R. S.; Andruski, S. W.; Broeker, J. L. *Rev. Heteroatom Chem.* **1988**, *1*, 31. Glass, R. S.; Andruski, S. W.; Broeker, J. L.; Firouzabadi, H.; Steffen, L. K.; Wilson, G. S. *J. Am. Chem. Soc.* **1989**, *111*, 4036. Glass, R. S.; Adamowicz, L.; Broeker, J. L. *J. Am. Chem. Soc.* **1991**, *113*, 1065. (b) Fujihara, H.; Ishitani, H.; Takaguchi, Y.; Furukawa, N. *Chem. Lett.* **1995**, 571. (c) Ernst, L.; Ibrom, K.; Chiu, J.-J.; Furukawa, N. *Tetrahedron Lett.* **1991**, *32*, 4345. Furukawa, N.; Fujii, T.; Kimura, T.; Fujihara, H. *Chem. Lett.* **1994**, 1007. (d) Nakanishi, W. *Chem. Lett.* **1993**, 2121.
- (8) (a) Nakanishi, W.; Hayashi, S.; Toyota, S. *J. Org. Chem.* **1998**, *63*, 8790. (b) Nakanishi, W.; Hayashi, S.; Toyota, S. *J. Chem. Soc., Chem. Commun.* **1996**, 371.
- (9) Regular and inverse substituent effects on $\delta(^1\text{Se})$ via $\delta(^8\text{Se})$ are reported in 1-(MeSe)-8-(*p*-YC₆H₄Se)C₁₀H₆ and 1-[8-(*p*-YC₆H₄Se)C₁₀H₆]-SeSe[C₁₀H₆(SeC₆H₄Y-*p*)-8']-1' (Y = H, OMe, Me, Cl, Br, CO₂Et, NO₂), respectively. See ref 3.
- (10) (a) Pimentel, G. C. *J. Chem. Phys.* **1951**, *19*, 446. Musher, J. I. *Angew. Chem., Int. Ed. Engl.* **1969**, *8*, 54. (b) Chen, M. M. L.; Hoffmann, R. *J. Am. Chem. Soc.* **1976**, *98*, 1647. (c) Cahill, P. A.; Dykstra, C. E.; Martin, J. C. *J. Am. Chem. Soc.* **1985**, *107*, 6359. See also, Hayes, R. A.; Martin, J. C. *Sulfurane Chemistry*. In *Organic Sulfur Chemistry: Theoretical and Experimental Advances*; Bernardi, F., Csizmadia, I. G., Mangini, A., Eds.; Elsevier: Amsterdam, 1985; Chapter 8.
- (11) (a) Nakanishi, W.; Hayashi, S.; Kihara, H. *J. Org. Chem.* **1999**, *64*, 2630.
- (12) Rosenfield, Jr., R. E.; Parthasarathy, R.; Dunitz, J. D. *J. Am. Chem. Soc.* **1977**, *99*, 4860.
- (13) Ramasubbu, N.; Parthasarathy, R. *Phosphorus Sulfur* **1987**, *31*, 221.
- (14) Frisch, M. J.; Trucks, G. W.; Schlegel, H. B.; Gill, P. M. W.; Johnson, B. G.; Robb, M. A.; Cheeseman, J. R.; Keith, T.; Petersson, G. A.; Montgomery, J. A.; Raghavachari, K.; Al-Laham, M. A.; Zakrzewski, V. G.; Ortiz, J. V.; Foresman, J. B.; Cioslowski, J.; Stefanov, B. B.; Nanayakkara, A.; Challacombe, M.; Peng, C. Y.; Ayala, P. Y.; Chen, W.; Wong, M. W.; Andres, J. L.; Replogle, E. S.; Gomperts, R.; Martin, R. L.; Fox, D. J.; Binkley, J. S.; Defrees, D. J.; Baker, J.; Stewart, J. P.; Head-Gordon, M.; Gonzalez, C.; Pople, J. A. *Gaussian94, Revision D.4*; Gaussian, Inc., Pittsburgh, PA, 1995.
- (15) These results are essentially the same as those reported in ref 8a. The calculations were performed on a model of **1** with the MP2/6-311++G-(3df,2pd) method. The Se...Se distance of the model was fixed at 3.053 Å and the two Se-H_b bonds were placed on the *xy*-plane and the two Se-H_a bonds were placed on the planes which cross the *xy*-plane at a right angle. The four Se-H bonds and the two HSeH angles and the two SeSeH angles were optimized. The optimized $\angle\text{SeSeH}$ values were 72.72° and 157.43°, respectively.
- (16) HOMO-*n* ($n = 2 - 5$) were also plotted against θ_1 . The energy curves are flat or change only monotonically.
- (17) Hehre, H. J. MacSpartan Plus Ver. 1.0, Wavefunction Inc.
- (18) The results of the MO calculations for 1-naphthaleneselenol will be reported elsewhere.
- (19) Glendening, E. D.; Reed, A. E.; Carpenter, J. E.; Weinhold, F. NBO Ver. 3.1.
- (20) Topson, R. D. The Nature and Analysis of Substituent Electronic Effects. In *Progress in Physical Organic Chemistry*; Taft, R. W., Ed.; John Wiley & Sons: New York, 1976; Vol. 12. See also refs cited therein.
- (21) The contribution of the $n(\text{Z})\cdots n(\text{Z})$ π type 2c-4e interaction (type C pairing) is important to the structures of 1,8-bis(alkyl(or aryl)chalcogena)-naphthalenes, which may be due to the same atoms (usually same groups) substituted at the 1,8-positions.
- (22) The interaction between the filled p type lone pair orbital of the Se atom and the p-type orbital of Y through the π orbitals of the aryl group must play an important role to determine the structure of **2** and **3**.²³
- (23) Studies on the structures of 1-(*p*-anisylselanyl)naphthalene (**11**) and 1-(*p*-chlorophenylselanyl)naphthalene (**12**), together with other Y in 1-(*p*-YC₆H₄Se)C₁₀H₇, are in progress in our laboratory. The conformations around the Se-C_{An} bond in **2** and the Se-C_{Ar} bond in **3** are close to those in **11** and **12**, respectively. Details on the structures of 1-(*p*-YC₆H₄Se)C₁₀H₇ will be reported elsewhere.
- (24) Beurskens, P. T.; Admiraal, G.; Beurskens, G.; Bosman, W. P.; Garcia-Granda, S.; Gould, R. O.; Smits, J. M. M.; Smykalla, C. The DIRDIF program system, Technical Report of the Crystallography Laboratory, University of Nijmegen, The Netherlands, 1992.
- (25) Beurskens, P. T.; Admiraal, G.; Beurskens, G.; Bosman, W. P.; de Gelder, R.; Israel, R.; Smits, J. M. M. The DIRDIF-94 program system, Technical Report of the Crystallography Laboratory, University of Nijmegen, The Netherlands, 1994.